



## Original Articles

# FOXF2 deficiency permits basal-like breast cancer cells to form lymphangiogenic mimicry by enhancing the response of VEGF-C/VEGFR3 signaling pathway

Qing-Shan Wang<sup>a, d</sup>, Rui He<sup>a</sup>, Fan Yang<sup>a</sup>, Li-Juan Kang<sup>a</sup>, Xiao-Qing Li<sup>a, d</sup>, Li Fu<sup>b, d</sup>, Baocun Sun<sup>c, \*\*</sup>, Yu-Mei Feng<sup>a, d, \*</sup>

<sup>a</sup> Department of Biochemistry and Molecular Biology, Tianjin Medical University Cancer Institute and Hospital, National Clinical Research Center of Cancer, China

<sup>b</sup> Department of Breast Pathology, Tianjin Medical University Cancer Institute and Hospital, National Clinical Research Center of Cancer, China

<sup>c</sup> Department of Pathology, Tianjin Medical University Cancer Institute and Hospital, National Clinical Research Center of Cancer, China

<sup>d</sup> Key Laboratory of Breast Cancer Prevention and Treatment of the Ministry of Education, Tianjin Medical University Cancer Institute and Hospital, National Clinical Research Center of Cancer, China



## ARTICLE INFO

## Article history:

Received 17 October 2017

Received in revised form

19 January 2018

Accepted 27 January 2018

## Keywords:

FOXF2

VEGFR3

Lymphangiogenic mimicry

Lymphatic metastasis

Basal-like breast cancer

## ABSTRACT

Lymphatic metastasis is the main route of breast cancer metastasis. It is known that lymphangiogenesis facilitates lymphatic metastasis through vascular endothelial growth factor-C (VEGF-C)/VEGF receptor 3 (VEGFR3) pathway-linked interactions between the tumor and its microenvironment. Here, we report a novel mechanism of lymphatic metastasis by which aggressive basal-like breast cancer (BLBC) cells form lymphatic vessel-like structures that are identified by the positive expression of lymphatic endothelial cell markers lymphatic vessel endothelial hyaluronan receptor 1 (LYVE-1), podoplanin, and VEGFR3, and termed as lymphangiogenic mimicry (LM), for the first time. Our clinical evidence and experimental data *in vivo* and *in vitro* revealed that forkhead box F2 (FOXF2) deficiency promotes the lymphatic metastasis of BLBC by conferring a lymphangiogenic mimetic feature upon cancer cells through directly activating VEGFR3 transcription. The fact that FOXF2 controls the activation of the VEGF-C/VEGFR3 signaling pathway in BLBC cells provides potential molecular diagnostic and therapeutic strategies for lymphatic metastasis in BLBC patients.

© 2018 Elsevier B.V. All rights reserved.

## 1. Introduction

Metastasis is the major cause of cancer-related death [1]. The majority of epithelial cancers often firstly metastasize to regional lymph nodes *via* lymphatic vessels [1,2]. Lymphatic vessel density in primary tumors correlates with lymph node metastasis and worse survival rates in cancer patients [3]. Tumor lymphangiogenesis, which is the formation of new lymphatic vessels within or

surrounding the primary tumor, facilitates lymphatic and distant metastasis [4]. Thus, studies clarifying the cellular and molecular mechanisms of tumor lymphangiogenesis would benefit the development of anticancer strategies.

For tumor lymphangiogenesis, the cells have been shown to originate from not only lymphatic endothelial cells (LECs) preexisting in lymphatic vessels in primary tumors [5] but also from tumor-associated macrophages (TAMs) in the tumor microenvironment which have integrated into the existing lymphatic structure [6]. The vascular endothelial growth factor-C (VEGF-C)/vascular endothelial growth factor receptor 3 (VEGFR3) axis is the pivotal pathway for lymphangiogenesis [5]. Physiologically, the tyrosine kinase receptor VEGFR3 (also known as FLT4) on LECs is activated by its specific ligand, VEGF-C, leading to the promotion of LEC proliferation, migration, and survival and the formation of new lymphatic vessels [7]. In tumor microenvironment, increased VEGF-C expression derived from cancer cells [8,9] or TAMs [10] has

\* Corresponding author. Department of Biochemistry and Molecular Biology, Tianjin Medical University Cancer Institute and Hospital, Huan-Hu-Xi Road, He-Xi District, Tianjin 300060, China.

\*\* Corresponding author. Department of Pathology, Tianjin Medical University Cancer Institute and Hospital, Huan-Hu-Xi Road, He-Xi District, Tianjin 300060, China.

E-mail addresses: [sunbaocun@aliyun.com](mailto:sunbaocun@aliyun.com) (B. Sun), [yymfeng@tmu.edu.cn](mailto:yymfeng@tmu.edu.cn) (Y.-M. Feng).

been identified. VEGFR3 also has been showed to be expressed on LECs [11], TAMs [6] or cancer cells [9,12]. VEGF-C expression is correlated with VEGFR3 expression in various types of human cancer tissues [13,14]. Patients with tumors expressing high levels of VEGF-C and VEGFR3 tend to suffer lymph node metastasis and worse survival [12]. Therefore, tumor lymphangiogenesis is involved in complicated cellular and molecular mechanisms that depend on the context of interactions among cancer cells, LECs and TAMs in a paracrine or autocrine manner [15]. It is well known that lymphangiogenesis is produced predominately by VEGFR3-expressing cells that have undergone VEGF-C induction [5]. VEGFR3 expressed on cancer cells confers the capabilities of growth, invasion and metastasis upon the cells [9,12]. However, little is known about how VEGFR3 expression is triggered in cancer cells; whether and how cancer cells expressing VEGFR3 contribute to tumor lymphangiogenesis remain unknown.

Our group recently reported that forkhead box F2 (FOXF2), a mesenchymal transcription factor, is specifically expressed in triple-negative breast cancer (TNBC)/basal-like breast cancer (BLBC) cells but not in non-BLBC cells, and FOXF2 deficiency promotes BLBC metastasis by activating the transcription of epithelial-mesenchymal transition-inducing transcription factors (EMT-TFs) *TWIST1* and *FOXO2* [16,17]. In this study, we extended the role and mechanism of FOXF2 in BLBC metastasis. We demonstrated that *VEGFR3* is a novel target gene of FOXF2, and FOXF2 represses *VEGFR3* transcription by directly binding to *VEGFR3* promoter in BLBC cells. FOXF2 deficiency promotes the lymphatic metastasis of BLBC cells by conferring a LEC-like feature upon the cells through activating *VEGFR3* transcription. BLBC cells with low FOXF2 expression can form lymphatic vessel-like structure that was termed as lymphangiogenic mimicry (LM), for the first time to our knowledge. LM formed by the aggressive cancer cells could provide channels for themselves to enter the lymphatic vessels that result in lymphatic metastases. The forced expression of FOXF2 controls the formation of LM through blocking the VEGF-C/VEGFR3 signaling pathway in BLBC cells.

## 2. Materials and methods

### 2.1. Breast cancer tissue specimens

A total of 34 primary TNBC tissue specimens were obtained from patients who underwent breast surgery at Tianjin Medical University Cancer Institute and Hospital (TMUCIH; Tianjin, China). The use of these specimens was approved by the Institutional Review Board of TMUCIH, and written consent was obtained from all participants. These cases were divided into lymph node negative (LN<sup>-</sup>; n = 14) and lymph node positive (LN<sup>+</sup>; n = 20) groups or N0 (n = 14), N1 (n = 13), N2 (n = 4) and N3 (n = 3) groups based on the lymph node metastatic status according to the TNM staging system of the American Joint Committee on Cancer. All cases were followed up for more than 3 years, and 30 cases were followed up for more than 5 years. Disease-free survival (DFS) was defined as the time interval between primary surgery and any relapse (local-regional, contra-lateral and/or distant) or the terminal time of follow-up without any relapse events.

### 2.2. Cells and treatment

The human breast cancer cell lines MCF-7, T47D, BT549, MDA-MB-231 and MDA-MB-231-luc-D3H2LN (231-Luc) were maintained in DMEM or RPMI 1640 medium (Invitrogen, Gaithersburg, MD, USA) supplemented with 10% fetal bovine serum (FBS), 100 units/mL penicillin, and 100 mg/mL streptomycin. For VEGF-C treatment, cells were treated with 50 ng/mL human recombinant

VEGF-C (R&D Systems, Inc., Minneapolis, MN, USA) and an equal volume of phosphate-buffered saline was used as a control.

### 2.3. Lentiviral transduction

231-Luc cells were infected with recombinant lentiviruses carrying human FOXF2 cDNA (LV-FOXF2), small hairpin RNA targeting FOXF2 (shFOXF2) or their negative controls LV-Vector and shControl (Genechem, Nanjin, China) and selected in 1.0 µg/mL puromycin for 2 weeks to establish cells stably expressing exogenous FOXF2 or silencing endogenous FOXF2.

### 2.4. Transfection of small interfering RNAs and plasmids

Small interfering RNAs (siRNAs) targeting the coding sequences of the FOXF2 or VEGFR3 genes (RiboBio Co., Guangzhou, China) are described in the supplemental material, Table S1. The human full-length FOXF2 cDNA (Genechem) was subcloned into the pcDNA3.1-FLAG vector (FOXF2-FLAG). Cells were transfected with siRNAs or plasmids using Lipofectamine 2000 (Invitrogen) according to the manufacturer's specifications.

### 2.5. Reverse transcription-quantitative PCR

Total RNA of tissues or cultured cells was isolated using TRIzol reagent (Invitrogen). Reverse transcription (RT) reaction was performed using a First-strand cDNA Synthesis System (Invitrogen) according to the manufacturer's instructions. We quantified the transcripts of the housekeeping gene glyceraldehyde 3-phosphate dehydrogenase (GAPDH) as an internal mRNA quantity control. Triplicate quantitative PCR reactions were performed for both target genes and the housekeeping gene using Platinum Quantitative PCR SuperMix-UDG System (Invitrogen) according to the manufacturer's instructions. The expression level of the target gene was calculated by normalizing the cycle threshold (Ct) values of the target gene to the Ct values of GAPDH ( $\Delta$ Ct), and determined as  $2^{-\Delta$ Ct}.

### 2.6. Immunoblot, immunohistochemistry, and immunofluorescence

For immunoblot, harvested cells were lysed with RIPA buffer supplemented with proteinase inhibitor cocktail (Sigma). A total of 30 µg protein lysate was separated by SDS-PAGE and then blotted onto a polyvinylidene difluoride membrane. After blocking in milk-based buffer, the membrane was incubated with primary antibody overnight at 4 °C followed by HRP-linked secondary antibodies. The immunoreactive protein bands on the membranes were visualized using chemiluminescence reagents (GE Healthcare).

Immunohistochemistry staining of formalin fixed and paraffin embedded tissue specimens were carried out using a primary antibody at appropriate concentration overnight at 4 °C. The bound antibody was detected using a peroxidase-conjugated secondary antibody. DAB substrate was used to perform the chromogenic reaction. The immunohistochemistry staining were quantified by multiplying the intensity scores with the extent of positivity scores of stained cancer cells, which were determined by two pathologists, who were blinded to patients' clinicopathologic characteristics and outcomes. The intensity scores were counted as 0, negative; 1, low; 2, medium; and 3, high. The extent of positivity scores were counted as 0, 0% stained; 1, 1–25% stained; 2, 26–50% stained; and 3, 51–100% stained. Then, the samples were divided into four grades according to the immunohistochemistry staining scores: negative (–) scored as 0, low staining (+) scored as 1–2; medium staining (++) scored as 3–5, and high staining (+++) scored as 6–9. And the patient were classed into high FOXF2 expression

(FOXF2<sub>high</sub>) group scored as ++/+++ and low FOXF2 expression (FOXF2<sub>low</sub>) group scored as -/+.

For immunofluorescence staining, frozen sections of xenograft tumors were fixed with cold acetone then treated by 0.1% Triton X-100 in PBS. The tissue sections were incubated with primary antibodies overnight at 4 °C followed by the appropriate secondary fluorescently labeled antibodies (Jackson ImmunoResearch Laboratories, USA). Nuclei were counterstained with DAPI (Thermo Fisher Scientific). Images were taken with fluorescence microscope (Zeiss).

The primary antibodies for immunoblot, immunohistochemistry and immunofluorescence are described in the supplemental material, Table S2.

### 2.7. ChIP-PCR assay

Chromatin immunoprecipitation (ChIP) assay was performed using a ChIP assay kit (EMD Millipore, Billerica, MA, USA) according to the manufacturer's instructions. Anti-FLAG antibody was used for immunoprecipitation to enrich the promoter fragments of *VEGFR3* gene in the cells transfected with plasmids expressing FLAG-tagged FOXF2. The primers used for the PCR amplification of ChIP-enriched *VEGFR3* promoter fragments are described in the supplemental material, Table S3.

### 2.8. Luciferase reporter assay

Luciferase reporter plasmids of the *VEGFR3* promoter region containing or lacking FOXF2 binding sites were established using the primers described in the supplemental material, Table S3. The fragments of the *VEGFR3* promoter were cloned into the luciferase reporter gene plasmid pGL3-Basic (Promega, Madison, WI, USA). The pGL3 reporter and pRL-TK plasmid were transiently co-transfected into cells for 48 h. The luciferase activity of pGL3 reporter was normalized to Renilla luciferase activity.

### 2.9. Cell invasion assay

Cell invasion capacities *in vitro* were assessed using Matrigel-coated transwell inserts (BD Biosciences, San Diego, CA, USA). A total of  $5 \times 10^4$  cells in 500  $\mu$ L serum-free medium were added to the upper chamber, and medium containing 20% FBS was added into the lower chamber. The cells were left to invade the Matrigel for the appropriate time, the non-invading cells on the upper surface of the membrane were removed by wiping, and the invading cells were fixed and stained with a three-step stain set kit (Richard-Allan Scientific, Waltham, MA, USA). The number of invading cells was counted under a microscope in five predetermined fields for each membrane at 200 $\times$  magnification.

### 2.10. Xenograft tumor assay

Female 4- to 6-week-old severe combined immunodeficiency (SCID) mice were injected into their left lower abdominal mammary fat pads with  $5 \times 10^6$  231-Luc cells infected with shFOXF2 (231-Luc-shFOXF2), shControl (231-Luc-shControl), LV-FOXF2 (231-Luc-LV-FOXF2) or LV-Vector (231-Luc-LV-Vector). For drug treatment, the xenograft mice were injected with 100  $\mu$ g/kg of VEGF-C or saline *via* the tail vein twice weekly for 3 weeks. For the evaluation of sentinel lymph node (SLN) metastasis, the xenograft mice were intratumorally injected with 200  $\mu$ L of 2.5  $\mu$ g/ $\mu$ L Patent Blue V dye (Sigma-Aldrich) and sacrificed for dissection to observe the collecting lymphatic vessels (CLVs) and metastatic lymph nodes at 10 min after the injection [18]. The bioluminescence imaging and data analysis, measurement of tumor volume and definition of

survival time of the xenograft mice were performed as previously described [17]. The primary tumors and lymph nodes were harvested from xenograft mice at sacrifice. The tissues were prepared for paraffin-embedded tissue sections and subjected to hematoxylin and eosin (H&E) staining or immunohistochemistry staining. Two independent experiments of xenograft-bearing mice were performed. In one experiment, the mice died naturally to enable calculations of the survival time. In the second experiment, the mice were sacrificed for dissection. Animal protocols performed in this work were approved by the Laboratory Animal Ethics Committee at TMUCIH.

### 2.11. Statistical analysis

Data from *in vitro* and *in vivo* experiments are presented as means  $\pm$  standard deviations (SD). Student's *t*-test was used to compare difference between the experimental and control groups, as well as the difference of the FOXF2 mRNA levels in primary tumors with different lymph node statuses. Fisher's exact test was used to compare the difference of lymph node metastasis incidence between different TNBC patient groups. Spearman's correlation analysis was used to analyze the correlation between FOXF2 mRNA levels and FOXF2 protein or *VEGFR3* mRNA levels in breast cancer tissues. Survival plots were created using Kaplan-Meier analysis, and log-rank test was used to assess statistical significance.  $P < 0.05$  was considered statistically significant.

## 3. Results

### 3.1. TNBC/BLBC cells form LM in primary tumors with low FOXF2 expression and lymph node metastases

To investigate the clinical relevance of FOXF2 expression with breast cancer lymphatic metastasis, we quantified FOXF2 mRNA levels in 34 primary TNBC tumors using RT-qPCR. The data revealed that FOXF2 mRNA levels in LN+ group ( $n = 20$ ) were lower than those in LN- group ( $n = 14$ ;  $P = 0.064$ ; Fig. 1A). Patients were further divided into N0 to N3 groups based on lymph node statuses, the difference of FOXF2 mRNA levels occurred between N0 and N2 or N3 groups ( $P = 0.036$ , N0 vs. N2-3), but did not occur between N0 and N1 groups (Fig. 1B). We then performed immunohistochemistry staining to detect FOXF2 protein expression in 31 TNBC tissue sections among the 34 cases. The immunohistochemistry staining scores of FOXF2 were significantly correlated with FOXF2 mRNA levels (Spearman's  $\rho = 0.365$ ,  $P = 0.043$ ; Fig. S1A and B). The lymphatic metastasis rate of the cases with FOXF2<sub>low</sub> (77.3%) was significantly higher than the cases with FOXF2<sub>high</sub> (11.1%; Fig. 1C). These pieces of clinical evidence indicate that FOXF2 expression negatively correlates with the lymphatic metastasis of TNBC/BLBC.

To further confirm the relationship between FOXF2 expression status and lymphatic metastasis in TNBC, we detected lymphatic vessels in the continuous sections of primary TNBC tissues by H&E and immunohistochemical staining. Surprisingly, we observed a strikingly interesting phenomenon: cancer cells in TNBC/BLBC tumors with low FOXF2 expression and lymph node metastases formed lymphatic vessel-like structures, which were identified by positive expression of the epithelial marker cytokeratin (CK) and the lymphatic endothelial cell markers podoplanin [19], *VEGFR3* [20] and LYVE-1 [21] (Fig. 1D). We also observed the LM structure in xenograft tumor of MDA-MB-231-Luc-shFOXF2 cells generated in our previous study [17] (Fig. 1E), while normal lymphatic vessels were positive for LYVE-1 and podoplanin but negative for CK (Fig. S1C). This clinical and experimental evidence implies that TNBC/BLBC cells with low FOXF2 expression could form a lymphatic-like vessel that was termed as LM for the first time. In

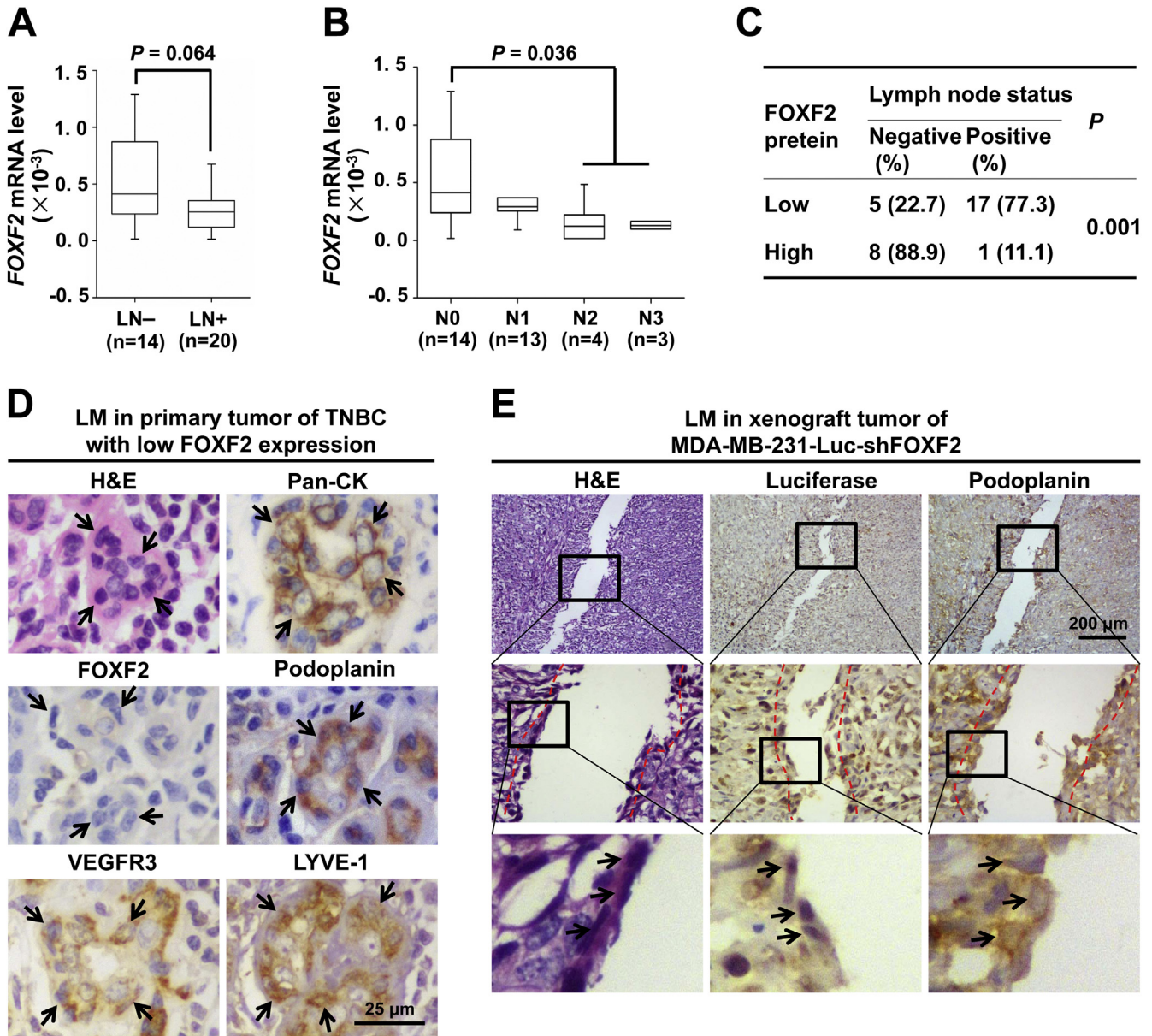


**Fig. 1.** TNBC cells form LM in primary tumors with low FOXF2 expression and lymph node metastasis. (A, B) Box plots comparing FOXF2 mRNA levels detected by RT-qPCR in primary tumors of TNBC patients (n = 34) with LN- and LN+ (A) and lymph node involvement statuses of N0 to N3 (B). (C) Table showing the incidence of lymphatic metastasis of TNBC cases with low and high FOXF2 expression according to immunohistochemistry staining. (D) H&E and immunohistochemistry staining for pan-CK, FOXF2, podoplanin, VEGFR3 and LYVE-1 in continuous sections of a primary TNBC tissue with low FOXF2 expression. Arrows indicate cancer cells in LM. (E) H&E and immunohistochemistry staining for luciferase and podoplanin expression in xenograft tumors. The selected areas are enlarged in the bottom panels. Dashed line indicates LM. Arrows indicate cancer cells in LM.

the continuous sections of a primary TNBC tissue, we also observed that tumor cells (CK+/VEGFR3+/LYVE-1+/podoplanin+) attached to or connected with LECs (CK-/VEGFR3+/LYVE-1+/podoplanin+) in the vessel structure to form a mosaic vessel that may facilitate the lymphatic metastasis of cancer cells (Fig. S2).

**3.2. FOXF2 deficiency promotes LM formation and lymphatic metastasis of BLBC cells in vivo**

To investigate the role of FOXF2 in lymphatic metastasis of BLBC cells, 231-Luc-shFOXF2 and 231-Luc-shControl cells were injected into the mammary fat pads of female SCID mice. The efficiency of FOXF2 knockdown is shown in Fig. S3A. We performed *in vivo* bioluminescence imaging to monitor metastasis using a Xenogen

IVIS system at day 18 post-injection. The bioluminescent imaging and metastatic photon flux analysis revealed that the 231-Luc-shFOXF2 mice displayed a greater extent of SLN metastasis than the control mice (Fig. 2A and B). To investigate the drainage function of lymphatic vessels in the primary tumor, Patent Blue V dye was injected intratumorally into mice bearing tumors [18], and then the mice were sacrificed for dissection at 10 min after injection. We observed that the Patent Blue V dye was drained into CLVs and SLNs in 50.0% (3/6) of 231-Luc-shFOXF2 mice, but not in the control mice (Fig. 2C and D). H&E staining revealed that 83.3% (5/6) of 231-Luc-shFOXF2 mice suffered SLN metastasis, whereas none of the control mice (0/6) suffered lymphatic metastasis (Fig. 2D and E). We further tested whether the lymphatic metastasis in 231-Luc-shFOXF2 mice is correlated with LM by immunofluorescence and

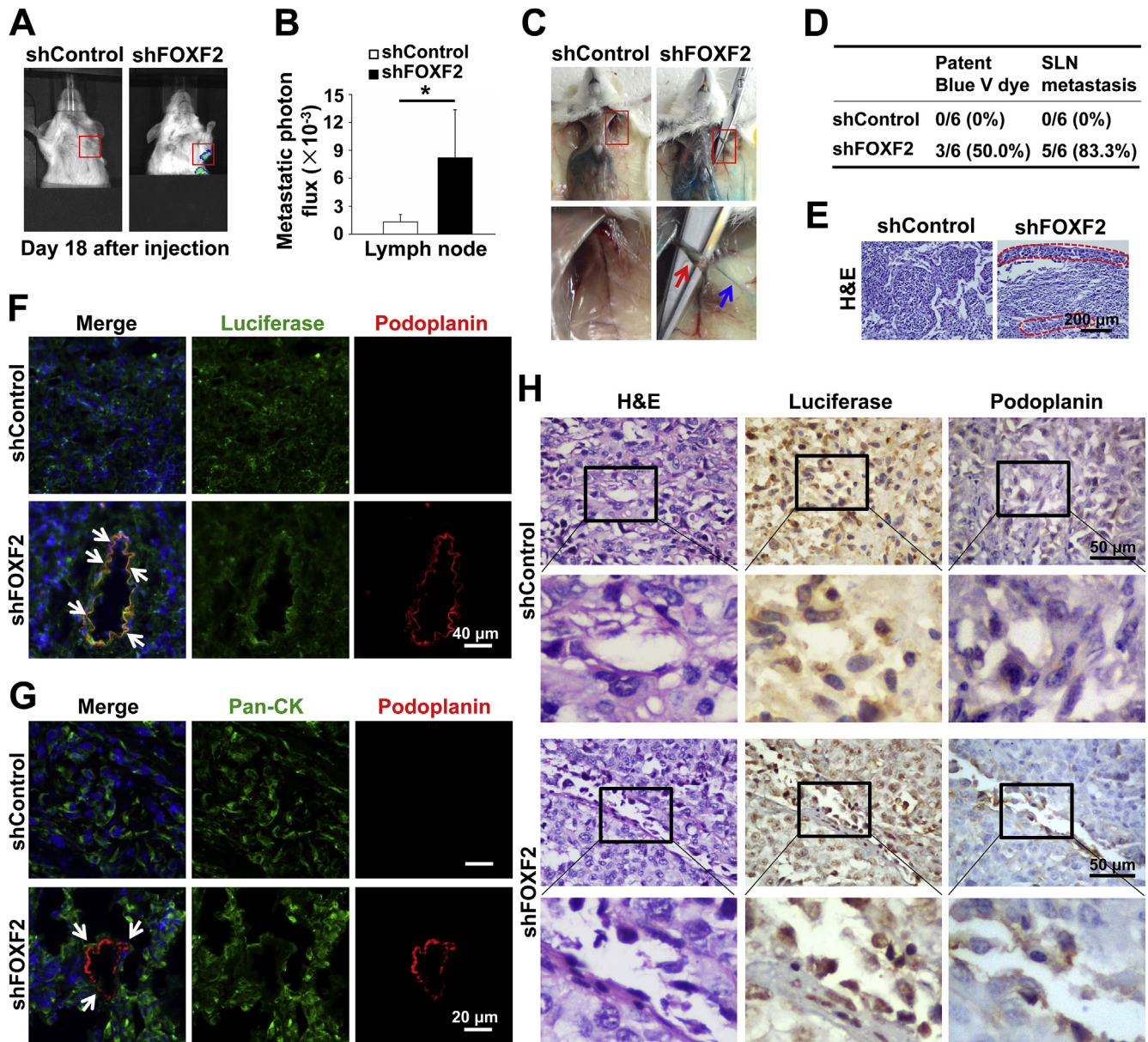


**Fig. 2.** FOXF2 deficiency promotes LM formation and lymphatic metastasis of BLBC cells *in vivo*. (A, B) Representative bioluminescence images (A) and the quantification of photon flux (B) of SLN metastasis of xenograft mice injected with 231-Luc-shFOXF2 cells ( $n = 6$ ) or 231-Luc-shControl cells ( $n = 6$ ). Red box indicates SLN. (C) Representative photos of the drainage of Patent Blue V dye to the CLVs and SLNs of xenograft mice. Blue arrow indicates drainage of Patent Blue V dye to the CLVs, and red arrow indicates drainage of Patent Blue V dye to the SLN. The selected areas are enlarged in the bottom panels. (D) Table showing the drainage of Patent Blue V dye to the CLVs and SLNs and the incidence of SLN metastasis in the mice bearing the indicated xenograft tumors. (E) H&E staining of SLN metastases harvested from xenograft mice. Dashed line marks metastasis. (F, G) Luciferase (F)/pan-CK (G) and podoplanin expression were detected by immunofluorescence staining in primary tumors harvested from mice bearing the indicated xenograft tumors. Arrow indicates LM. (H) H&E and immunohistochemistry staining for luciferase and podoplanin expression in primary tumors harvested from mice bearing the indicated xenograft tumors. The selected areas are enlarged in the bottom panels. Dashed line indicates LM. \* $P < 0.05$ .

immunohistochemical staining with anti-luciferase, anti-pan-CK, and anti-human podoplanin antibodies. We observed the tube structures formed by cancer cells with double-positive luciferase/pan-CK and podoplanin staining in the primary tumors of mice (Fig. 2F, G and H). LMs in 231-Luc-shFOXF2 tumors were significantly more than that in 231-Luc-shControl tumors (Fig. S4A and B), and immunofluorescence using anti-mouse podoplanin antibodies showed that normal lymphatic vessels in 231-Luc-shFOXF2 tumors were also significantly more than that in 231-Luc-shControl tumors (Fig. S4C). These pieces of *in vivo* evidence demonstrate that FOXF2 deficiency promotes LM formation and the lymphatic metastasis of BLBC cells.

### 3.3. FOXF2 binds to the VEGFR3 promoter and represses its transcription

Since VEGFR2- and VEGFR3-mediated pathways play pivotal roles in lymphangiogenesis [5,20], we speculated that the role of FOXF2 in the formation of LM is related to the expression of VEGFR2 or VEGFR3. Thus, we silenced or overexpressed FOXF2 in MDA-MB-231 and BT549 BLBC cells by transiently transfecting two independent siFOXF2 or FOXF2-FLAG. The results showed that FOXF2 knockdown significantly increased VEGFR3 expression in MDA-MB-231 cells (Fig. 3A), and FOXF2 overexpression decreased VEGFR3 expression in MDA-MB-231 and BT549 cells at both mRNA

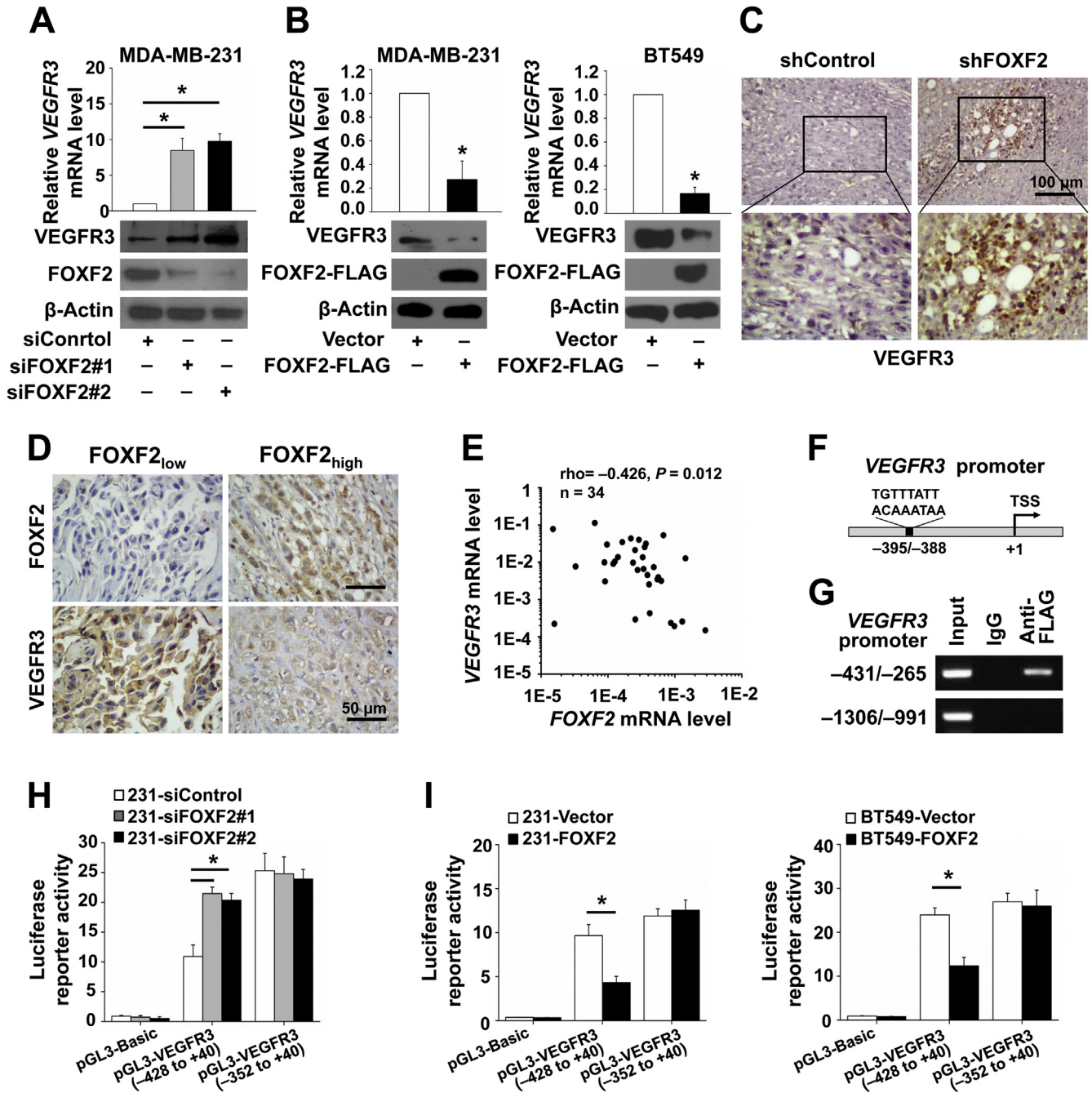


**Fig. 3.** FOXF2 binds to the *VEGFR3* promoter and represses its transcription. (A, B) The mRNA and protein levels of *VEGFR3* and *FOXF2* in the indicated cells were measured by RT-qPCR and immunoblot, respectively. (C) *VEGFR3* expression detected by immunohistochemistry staining in primary tumors harvested from xenograft-bearing mice injected with 231-Luc-shFOXF2 cells or 231-Luc-shControl cells. The selected areas are enlarged in the bottom panels. (D) Representative images of immunohistochemistry staining for *FOXF2* and *VEGFR3* expression in TNBC tissues. (E) The correlation of *FOXF2* mRNA levels with *VEGFR3* mRNA levels in human primary TNBC tissues (n = 34; Spearman's correlation rho = -0.426, P = 0.012). (F) Schematic of putative FOXF2 binding site in the *VEGFR3* promoter region. (G) The binding of FOXF2 on the *VEGFR3* promoter region containing (-431 to -265 bp) or lacking (-1306 to -991 bp) putative binding site in MDA-MB-231 cells transfected with FOXF2-FLAG was tested by a ChIP-PCR assay using anti-FLAG antibody. IgG was used as a negative control. (H, I) The transcriptional activity of the *VEGFR3* promoter in the indicated cells was assessed using a Dual-Luciferase Reporter Assay System. Data represent the mean ± SD of two independent experiments performed in triplicate. \*P < 0.05.

and protein levels (Fig. 3B). Immunohistochemistry staining showed that the primary tumors in 231-Luc-shFOXF2 mice expressed higher levels of *VEGFR3* than those in control mice (Fig. 3C). The clinical data confirmed that TNBC tissues with low FOXF2 expression presented higher *VEGFR3* expression (Fig. 3D) and *VEGFR3* mRNA levels inversely correlated with the FOXF2 mRNA levels in 34 cases of primary TNBC tumors (Spearman's

rho = -0.426, P = 0.012; Fig. 3E). However, the alteration of FOXF2 expression did not affect *VEGFR2* expression in MDA-MB-231 (Fig. S5A and B) and BT549 cells (undetectable). Thus, the role of FOXF2 in regulating LM formation may be only related to *VEGFR3* expression.

Therefore, we investigated whether *VEGFR3* is a transcriptional target of FOXF2. We performed a BLAST search for FOXF2 binding

sequences in the promoter region of the *VEGFR3* gene. We found a putative FOXF2 binding site in the *VEGFR3* promoter region from –395 bp to –388 bp relative to the transcription start site (TSS; Fig. 3F). Subsequently, the binding of FOXF2 on the *VEGFR3* promoter region containing the putative binding site was verified by a ChIP-PCR assay in MDA-MB-231 cells (Fig. 3G). To further assess the regulatory activity of FOXF2 on the *VEGFR3* promoter, we performed luciferase reporter assays by co-transfecting pGL3-*VEGFR3* –428/+40 containing the FOXF2 binding site or pGL3-*VEGFR3* –352/+40 lacking the binding site with siFOXF2, FOXF2-FLAG or their controls into MDA-MB-231 and BT549 cells. The results showed that FOXF2 knockdown increased the reporter activity of pGL3-*VEGFR3* –428/+40 in MDA-MB-231 cells, whereas it did not affect the reporter activity of pGL3-*VEGFR3* –352/+40 (Fig. 3H). Conversely, FOXF2 overexpression in MDA-MB-231 and BT549 cells decreased the reporter activity of pGL3-*VEGFR3* –428/+40, but not that of pGL3-*VEGFR3* –352/+40 (Fig. 3I). These results demonstrate that FOXF2 represses the transcriptional activity of the *VEGFR3* promoter by binding to the site at –395 to –388 bp.

#### 3.4. FOXF2 controls the phenotypic conversion of BLBC cells into lymphatic endothelial-like feature through blocking the VEGF-C/*VEGFR3* signaling pathway

Because FOXF2 represses *VEGFR3* transcription in BLBC cells, we next investigated whether FOXF2 controls the VEGF-C/*VEGFR3* signaling pathway in the LM formation of BLBC cells. We performed FOXF2 gain- or loss-of-function experiments in MDA-MB-231 and BT549 cells. We found that FOXF2 knockdown enhanced the invasion (Fig. 4A) of MDA-MB-231 cells, as well as the expression of LYVE-1 and podoplanin (Fig. 4C). *VEGFR3* knockdown (Fig. S3B) abrogated the effects of FOXF2 knockdown (Fig. 4A and C). Conversely, FOXF2 overexpression abolished the inducing role of VEGF-C signaling for invasion of MDA-MB-231 and BT549 cells (Fig. 4B), as well as suppressed the increased expression of podoplanin (only MDA-MB-231 cells) and LYVE-1 by VEGF-C induction (Fig. 4D). These results suggest that FOXF2 deficiency promote BLBC cells to phenotypically convert into lymphatic endothelial-like cells by activating the VEGF-C/*VEGFR3* signaling pathway through transcriptionally increasing *VEGFR3* expression. In addition, VEGF-C could not induce luminal breast cancer cell lines MCF-7 and T47D cells to express lymphatic endothelial cell markers (Fig. S7). Thus, luminal breast cancer cells have nocapacity to convert into lymphatic endothelial-like cells.

#### 3.5. FOXF2 inhibits LM formation and lymphatic metastasis in vivo

To investigate the roles of FOXF2 and the VEGF-C/*VEGFR3* signaling pathway in LM formation and lymphatic metastasis *in vivo*, 231-Luc, 231-Luc-LV-FOXF2 or 231-Luc-LV-Vector cells were injected into the mammary fat pads of female SCID mice. The mice received twice-weekly injections of 100 µg/kg VEGF-C or saline for 3 weeks. Bioluminescent imaging and metastatic photon flux analyses revealed that the mice with VEGF-C treatment suffered more SLN metastases than the control mice at 39 days after injection (Fig. 5A and B). Consistently, the 231-Luc tumor-bearing mice treated with VEGF-C displayed worse survival rates than the control mice (Fig. 5C). When the mice were sacrificed for dissection, we observed that the drainage of Patent Blue V dye from the primary tumor to the SLNs in mice treated with VEGF-C (4/6) was significantly more than that in control mice (0/6; Fig. 5D and E). H&E staining confirmed that the mice with VEGF-C treatment suffered more severe lymphatic metastasis (5/6) than the control mice (1/6; Fig. 5E and F). We also observed tube structures with luciferase and human podoplanin double-positive expression in the primary

tumors from the VEGF-C-treated mice (Figs. 5G and 6A). FOXF2 overexpression in 231-Luc cells reversed all of above effects of VEGF-C treatment (Fig. 5A–G and 6A). These results suggest that the VEGF-C/*VEGFR3* signaling pathway promotes LM formation and lymphatic metastasis of BLBC cells, while normal or high FOXF2 expression in BLBC cells could protect the cells from obtaining lymphatic metastatic capacity through blocking the VEGF-C/*VEGFR3* signaling pathway. These pieces of *in vivo* evidence further confirm that the FOXF2/*VEGFR3* regulatory axis controls the lymphatic metastasis and aggressive progression of BLBC cells.

#### 3.6. Combined detection of FOXF2 and *VEGFR3* mRNA levels effectively reflects the lymph node metastasis and DFS statuses of TNBC patients

Based on the facts that the patients with lymph node metastasis have worse prognosis, and FOXF2 and *VEGFR3* play opposite roles in lymphatic metastasis, we next addressed whether the combined detection of FOXF2 and *VEGFR3* mRNA levels could effectively predict lymph node metastasis and prognosis in TNBC/BLBC patients. Thus, we grouped the 34 cases of TNBC patients into four groups based on their FOXF2 and *VEGFR3* mRNA levels: FOXF2<sub>high</sub>/*VEGFR3*<sub>low</sub>, FOXF2<sub>high</sub>/*VEGFR3*<sub>high</sub>, FOXF2<sub>low</sub>/*VEGFR3*<sub>high</sub>, and FOXF2<sub>low</sub>/*VEGFR3*<sub>low</sub>. Our clinical data showed that patients in the FOXF2<sub>high</sub>/*VEGFR3*<sub>low</sub> and FOXF2<sub>low</sub>/*VEGFR3*<sub>high</sub> groups had the best and worst lymph node involvement and DFS statuses, respectively, and patients in the FOXF2<sub>high</sub>/*VEGFR3*<sub>high</sub> and FOXF2<sub>low</sub>/*VEGFR3*<sub>low</sub> groups had moderate lymph node involvement and DFS statuses compared to the other two groups (Fig. 6B and C). This clinical evidence further supports the negatively regulatory role of FOXF2 for the VEGF-C/*VEGFR3* signaling pathway in TNBC/BLBC cells and indicates that the combined detection of FOXF2 and *VEGFR3* mRNA levels effectively reflects lymph node metastasis and DFS statuses in TNBC patients.

## 4. Discussion

Distant metastasis is raised by the spread of cancer cells that access blood and lymphatic vascular systems. Tumor angiogenesis and lymphangiogenesis have similar cellular and molecular mechanisms that depend on interactions between the VEGF isoforms derived from cancer cells [8,9] or macrophages [10] and VEGFRs on preexisting vascular endothelial cells (VECs) [22] and LECs [11], or macrophages [23] in the tumor microenvironment. Vasculogenic mimicry (VM), vessel-like structures formed by aggressive tumor cells, has been defined [24] and well investigated. However, whether and how cancer cells expressing *VEGFR3* contribute to tumor lymphangiogenesis and even form LM, which may be similar to VM, remain unknown. In the current study, we observed a phenomenon of LM in clinical samples. Cancer cells in TNBC/BLBC tumors with low FOXF2 expression and lymph node metastases could form lymphatic vessel-like structures that were identified by the positive expression of lymphatic endothelial cell markers *VEGFR3*, LYVE-1, and podoplanin.

Interestingly, we observed that in a vessel structure, tumor cells (CK+/*VEGFR3*+/*LYVE-1*+/*podoplanin*+) attached to or connected with LECs (CK–/*VEGFR3*+/*LYVE-1*+/*podoplanin*+) to form a mosaic vessel that may facilitate the lymphatic metastasis of cancer cells (Fig. S2). Further *in vivo* and *in vitro* experiments confirmed that FOXF2 deficiency permits BLBC cells to form LM by enhancing the response of the VEGF-C/*VEGFR3* signaling pathway. These pieces of evidence imply that LM formed by aggressive cancer cells could provide channels for themselves to enter the lymphatic vessels that accelerate lymphatic metastases. In addition, aggressive cancer cells that have undergone EMT are carrying stem-like

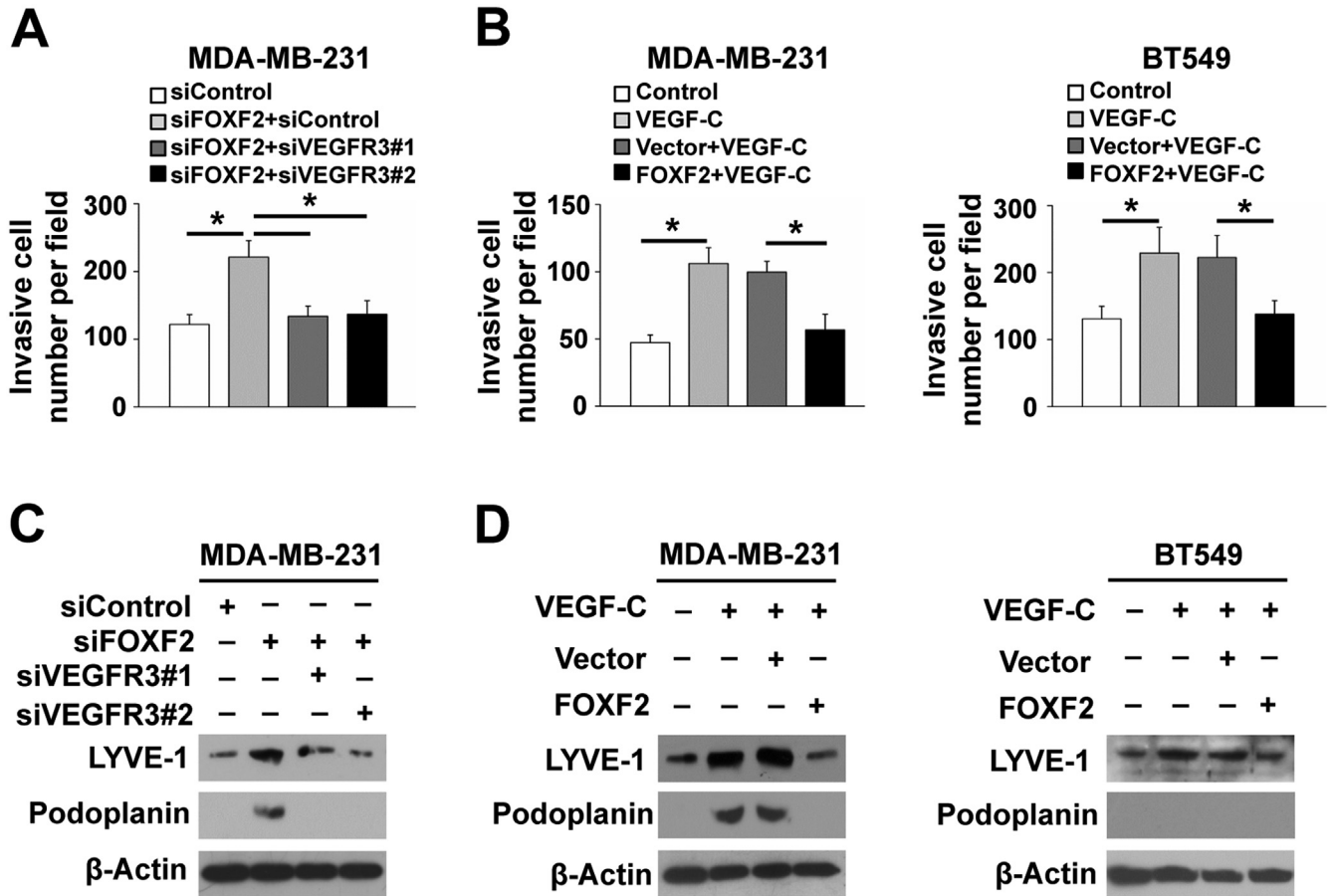


**Fig. 4.** FOXF2 controls the conversion of BLBC cells into an LEC-like feature through blocking the VEGF-C/VEGFR3 signaling pathway. (A, B) The invasion abilities of the indicated cells were assessed by transwell assay. Data represent the mean ± SD of two independent experiments performed in duplicate. \**P* < 0.05. (C, D) The protein expression levels of LYVE-1 and podoplanin in the indicated cells were detected by immunoblot.

characteristics with plasticity. These cells can be induced into multi-directional *trans*-differentiation in the tumor microenvironment, e.g., vascular endothelial cells [25,26], vascular pericytes [27,28], osteoblasts [29,30], myofibroblasts [31], and macrophages [32]. In the current study, we show that FOXF2-deficient BLBC cells that have undergone EMT [16,17] could be also induced into lymphatic differentiation by VEGF-C in the tumor microenvironment.

Axillary lymph node metastasis is the most important poor prognostic factor for patients with primary breast cancer. In particular, patients with four or more involved nodes at initial diagnosis have a significantly worse outcome after relapse than node-negative cases [33]. Our clinical data revealed that TNBC tumors with low FOXF2 expression tended to develop four or more involved nodes than those with high FOXF2 expression. Combined with our previous reports that FOXF2 deficiency promotes the EMT of BLBC cells by activating TWIST1 and FOXC2 transcription and the fact that BLBC cells with low FOXF2/FOXC2 expression could form LM, these findings indicate that only cancer cells that acquired aggressive behaviors and established primary lymphatic invasion can interact with LECs and were educated by the tumor-associated LECs to convert into a LEC-like phenotype in the tumor microenvironment.

VEGFR3 is an essential mediator of tumor lymphangiogenesis for LECs [34] and TAMs [6], as well as the formation of LM by aggressive cancer cells. Understanding of the mechanism regulating VEGFR3 expression would benefit the development of

targeted therapeutic strategies for blocking tumor lymphangiogenesis. It has been reported that Snail, an EMT-TF, upregulates VEGFR3 mRNA expression by directly binding to the VEGFR3 promoter via cooperating with early growth response protein-1 [35]. In the present study, we demonstrated that FOXF2, an EMT-suppressing transcription factor in BLBC cells, downregulated VEGFR3 mRNA expression by directly binding to the VEGFR3 promoter. Interestingly, we previously reported that FOXF2 transrepressed multiple EMT-TFs in BLBC cells, including TWIST1 and FOXC2 [16,17]. FOXC2 is also recognized as an activator and marker of lymphangiogenesis [36–38]. These pieces of evidence indicate that FOXF2 may act as a key controller of LM formation through either directly repressing VEGFR3 expression or indirectly repressing the network of EMT-TFs in BLBC cells. Although the functions of FOXF2 in BLBC reported in the study by Lo et al. [39] and our studies [16,17,40,41] were contradictory, multiple reports from other groups consistent with our finding that decreased FOXF2 expression promotes the aggressiveness and metastasis of BLBC or other types of cancer [42–44]. This study further extends the mechanism of FOXF2 function in BLBC metastasis.

Our previous report showed that FOXF2 is expressed at high levels in BLBC cells but is less expressed in non-BLBC cells [17]. VEGFR3 expression has been found at lower levels in basal-like subtype breast cancers than in other subtypes [13]. These pieces of evidence reflect the negative regulatory effect of FOXF2 on the VEGF-C/VEGFR3 pathway. Our clinical evidence that FOXF2 and VEGFR3 mRNA levels were negatively correlated in primary TNBC

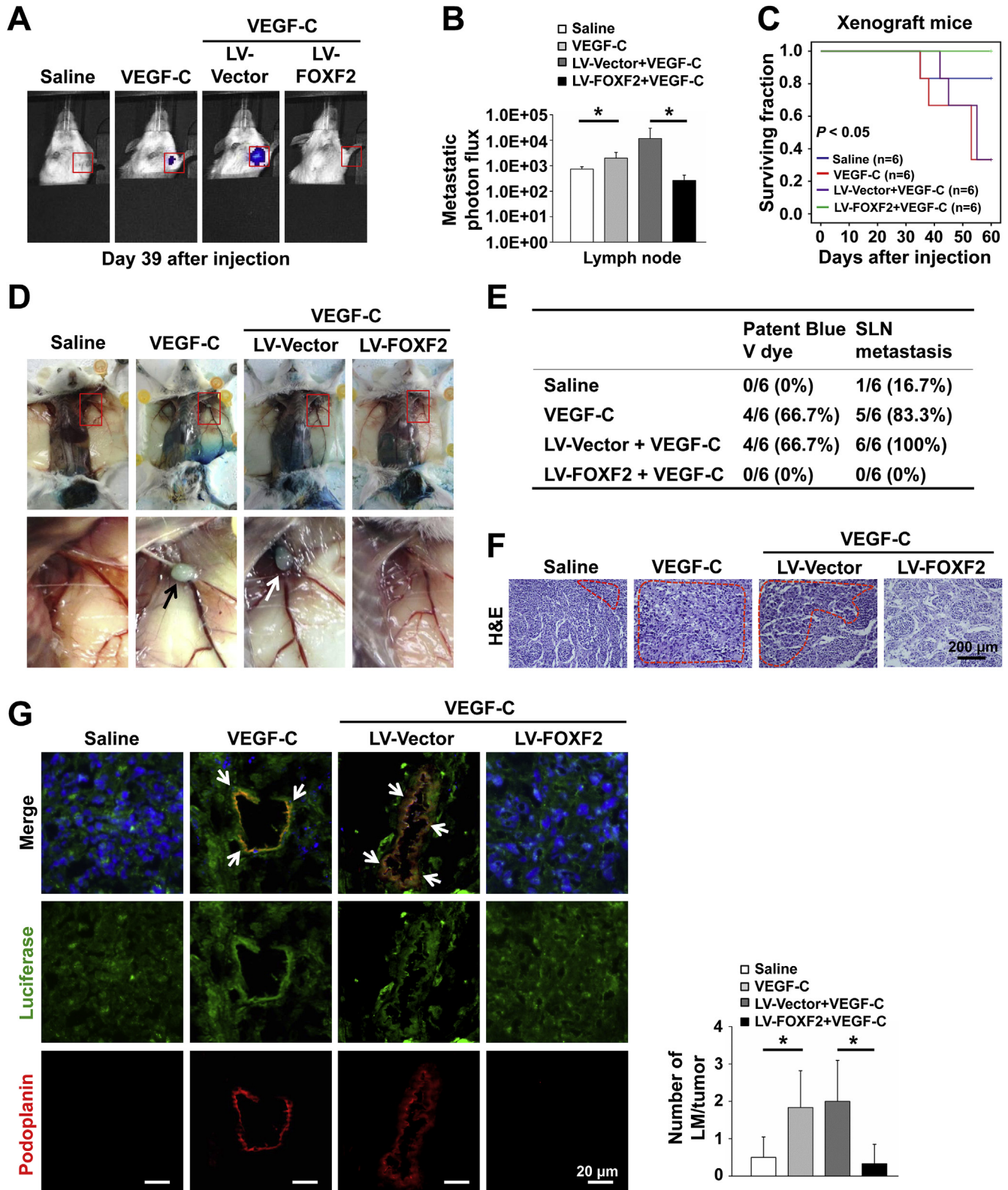


**Fig. 5.** FOXF2 inhibits LM formation and lymphatic metastasis *in vivo*. (A, B) Representative bioluminescence images (A) and the quantification of photon flux (B) of SLN metastasis of xenograft-bearing mice treated as indicated (n = 6). Red box indicates SLN. \*P < 0.05. (C) Kaplan–Meier curves of the overall survival of the indicated xenograft-bearing mice (n = 6). (D) Representative photos of the drainage of Patent Blue V dye to the SLNs of the indicated xenograft-bearing mice. Arrow indicates drainage of Patent Blue V dye to the SLNs. The selected areas are enlarged in the respective bottom panels. (E) Table showing the drainage of Patent Blue V dye to the SLNs and the incidence of SLN metastasis in the indicated xenograft-bearing mice. (F) H&E staining of SLN metastasis in the indicated xenograft-bearing mice. Dashed line indicates metastasis. (G) Luciferase and podoplanin expression was detected by immunofluorescence staining in primary tumors harvested from mice bearing the indicated xenograft tumors. Arrow indicates LM. Left, representative images of immunofluorescence staining for LM; right, the quantification of LMs in per section of primary tumors (n = 6). \*P < 0.05.

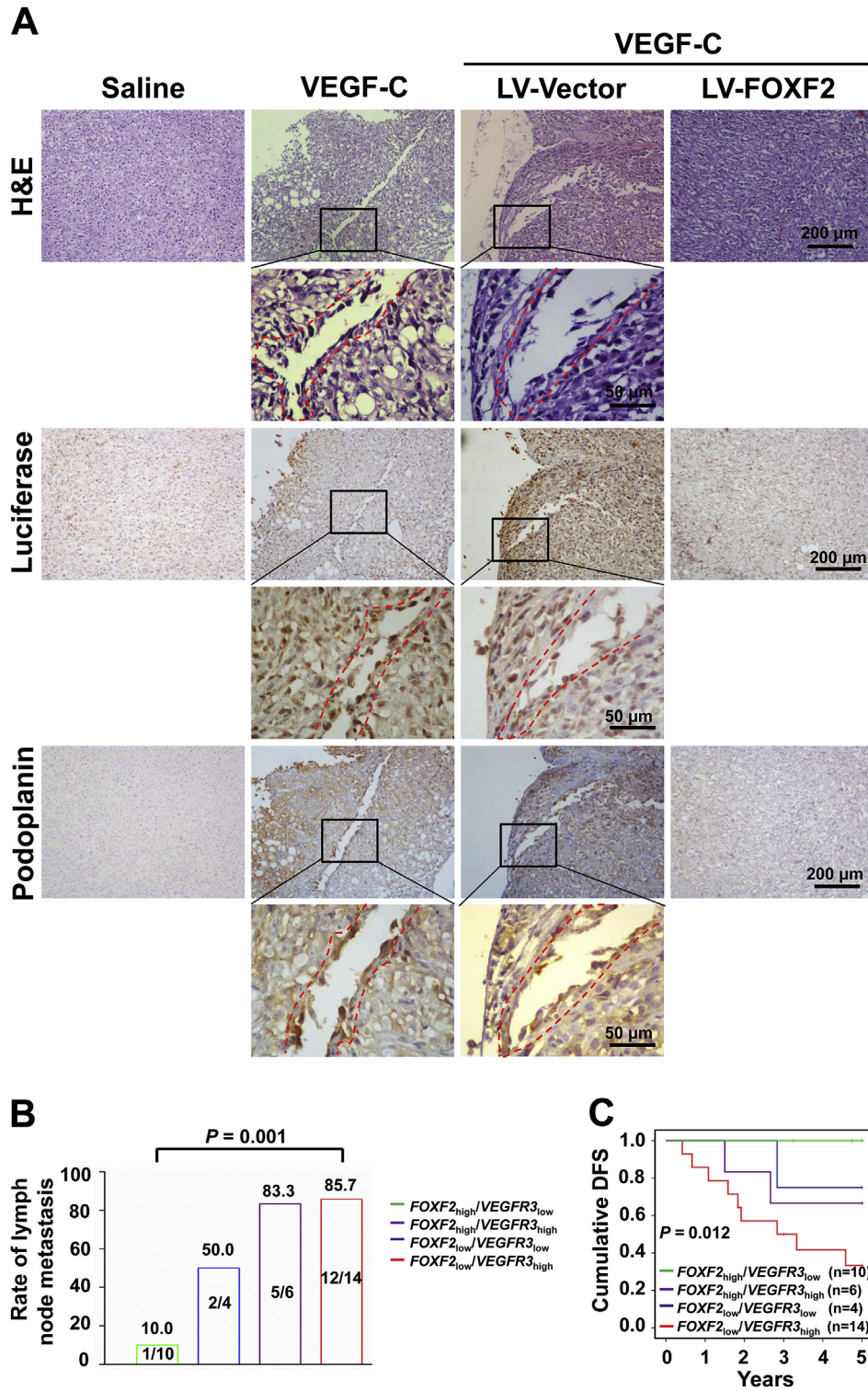


**Fig. 6.** FOXF2 inhibits LM formation *in vivo* and the combined detection of FOXF2 and VEGFR3 mRNA levels effectively reflects the lymph node involvement and DFS statuses of TNBC patients. (A) Luciferase and podoplanin expression were detected by immunohistochemistry staining in primary tumors harvested from mice bearing the indicated xenograft tumors. The selected areas are enlarged in the respective bottom panels. Dashed line indicates LM. (B) The incidence of lymphatic metastasis in TNBC patients with FOXF2<sub>high</sub>/VEGFR3<sub>low</sub> (n = 10), FOXF2<sub>high</sub>/VEGFR3<sub>high</sub> (n = 6), FOXF2<sub>low</sub>/VEGFR3<sub>low</sub> (n = 4) and FOXF2<sub>low</sub>/VEGFR3<sub>high</sub> (n = 14). (C) The correlation of the combined FOXF2 and VEGFR3 mRNA levels with the DFS of TNBC patients was estimated by Kaplan-Meier survival analysis.

tissues and conversely predicted lymph node metastasis and prognosis further supports the negative regulatory effect of FOXF2 on the VEGF-C/VEGFR3 signaling pathway during the lymphatic metastasis of TNBC/BLBC, and indicates that the combination of

FOXF2 and VEGFR3 mRNA levels is an effective prognostic predictor for TNBC patients.

In conclusion, we identified a novel cellular and molecular mechanism of lymphatic metastasis by which aggressive BLBC cells

form lymphatic vessel-like structures, termed as LM, for the first time. FOXF2 deficiency promotes the lymphatic metastasis of BLBC cells by conferring a LEC mimetic feature on cancer cells through directly activating *VEGFR3* transcription. The fact that FOXF2 controls the activation of the VEGF-C/VEGFR3 signaling pathway in BLBC cells provides potential molecular diagnostic and targeted therapeutic strategies for lymphatic metastasis of BLBC patients.

### Conflict of interest

The authors declare no conflict of interest.

### Grant sponsor

This work was supported by grants from the National Natural Science Foundation of China (Nos. 81272357, 81201652, 81472680, 81672894 and 81773125) and the National Science and Technology Support Project of China (No. 2015BAI12B15).

### Appendix A. Supplementary data

Supplementary data related to this article can be found at <https://doi.org/10.1016/j.canlet.2018.01.069>.

### References

- [1] S. Karaman, M. Detmar, Mechanisms of lymphatic metastasis, *J. Clin. Invest.* 124 (2014) 922–928.
- [2] S. Ran, K.E. Montgomery, Macrophage-mediated lymphangiogenesis: the emerging role of macrophages as lymphatic endothelial progenitors, *Cancers* 4 (2012) 618–657.
- [3] Y. Nakamura, H. Yasuoka, M. Tsujimoto, S. Imabun, M. Nakahara, K. Nakao, et al., Lymph vessel density correlates with nodal status, VEGF-C expression, and prognosis in breast cancer, *Breast Canc. Res. Treat.* 91 (2005) 125–132.
- [4] B. Garmy-Susini, C.J. Avraamides, J.S. Desgrosellier, M.C. Schmid, P. Foubert, L.G. Ellies, et al., PI3K $\alpha$  activates integrin  $\alpha 4 \beta 1$  to establish a metastatic niche in lymph nodes, *Proc. Natl. Acad. Sci. U. S. A.* 110 (2013) 9042–9047.
- [5] T. Tammela, K. Alitalo, Lymphangiogenesis: molecular mechanisms and future promise, *Cell* 140 (2010) 460–476.
- [6] A. Zumsteg, V. Baeriswyl, N. Imaizumi, R. Schwendener, C. Ruegg, G. Christofori, Myeloid cells contribute to tumor lymphangiogenesis, *PLoS One* 4 (2009), e7067.
- [7] T. Makinen, T. Veikkola, S. Mustjoki, T. Karpanen, B. Catimel, E.C. Nice, et al., Isolated lymphatic endothelial cells transduce growth, survival and migratory signals via the VEGF-C/D receptor VEGFR-3, *EMBO J.* 20 (2001) 4762–4773.
- [8] R. Shayan, M.G. Achen, S.A. Stacker, Lymphatic vessels in cancer metastasis: bridging the gaps, *Carcinogenesis* 27 (2006) 1729–1738.
- [9] M.L. Varney, R.K. Singh, VEGF-C-VEGFR3/Flt4 axis regulates mammary tumor growth and metastasis in an autocrine manner, *Am J Cancer Res.* 5 (2015) 616–628.
- [10] D. Moussai, H. Mitsui, J.S. Pettersen, K.C. Pierson, K.R. Shah, M. Suarez-Farinas, et al., The human cutaneous squamous cell carcinoma microenvironment is characterized by increased lymphatic density and enhanced expression of macrophage-derived VEGF-C, *J. Invest. Dermatol.* 131 (2011) 229–236.
- [11] T.T. Qin, G.C. Xu, J.W. Qi, G.L. Yang, K. Zhang, H.L. Liu, et al., Tumour necrosis factor superfamily member 15 (Tnfsf15) facilitates lymphangiogenesis via up-regulation of Vegfr3 gene expression in lymphatic endothelial cells, *J. Pathol.* 237 (2015) 307–318.
- [12] J.L. Su, P.C. Yang, J.Y. Shih, C.Y. Yang, L.H. Wei, C.Y. Hsieh, et al., The VEGF-C/Flt-4 axis promotes invasion and metastasis of cancer cells, *Canc. Cell* 9 (2006) 209–223.
- [13] M. Raica, A.M. Cimpean, R. Ceausu, D. Ribatti, Lymphatic microvessel density, VEGF-C, and VEGFR-3 expression in different molecular types of breast cancer, *Anticancer Res.* 31 (2011) 1757–1764.
- [14] S. Shushanov, M. Bronstein, J. Adelaide, L. Jussila, T. Tchipyshva, J. Jacquemier, et al., VEGF $\alpha$  and VEGFR3 expression in human thyroid pathologies, *Int J Cancer* 86 (2000) 47–52.
- [15] A. Alitalo, M. Detmar, Interaction of tumor cells and lymphatic vessels in cancer progression, *Oncogene* 31 (2012) 4499–4508.
- [16] J. Cai, A.X. Tian, Q.S. Wang, P.Z. Kong, X. Du, X.Q. Li, et al., FOXF2 suppresses the FOXC2-mediated epithelial-mesenchymal transition and multidrug resistance of basal-like breast cancer, *Canc. Lett.* 367 (2015) 129–137.
- [17] Q.S. Wang, P.Z. Kong, X.Q. Li, F. Yang, Y.M. Feng, FOXF2 deficiency promotes epithelial-mesenchymal transition and metastasis of basal-like breast cancer, *Breast Cancer Res.* 17 (2015) 30.
- [18] T. Karnezis, R. Shayan, C. Caesar, S. Roufai, N.C. Harris, K. Ardiapradja, et al., VEGF-D promotes tumor metastasis by regulating prostaglandins produced by the collecting lymphatic endothelium, *Canc. Cell* 21 (2012) 181–195.
- [19] J.T. Wigle, G. Oliver, Prox1 function is required for the development of the murine lymphatic system, *Cell* 98 (1999) 769–778.
- [20] W. Zheng, A. Aspelund, K. Alitalo, Lymphangiogenic factors, mechanisms, and applications, *J. Clin. Invest.* 124 (2014) 878–887.
- [21] S. Banerji, J. Ni, S.X. Wang, S. Clasper, J. Su, R. Tammi, et al., LYVE-1, a new homologue of the CD44 glycoprotein, is a lymph-specific receptor for hyaluronan, *J. Cell Biol.* 144 (1999) 789–801.
- [22] D. Tvorogov, A. Anisimov, W. Zheng, V.M. Leppanen, T. Tammela, S. Laurinavicius, et al., Effective suppression of vascular network formation by combination of antibodies blocking VEGFR ligand binding and receptor dimerization, *Canc. Cell* 18 (2010) 630–640.
- [23] C. Scavelli, B. Nico, T. Cirulli, R. Ria, G. Di Pietro, D. Mangieri, et al., Vasculogenic mimicry by bone marrow macrophages in patients with multiple myeloma, *Oncogene* 27 (2008) 663–674.
- [24] A.J. Maniotis, R. Folberg, A. Hess, E.A. Sefror, L.M. Gardner, J. Pe'er, et al., Vascular channel formation by human melanoma cells in vivo and in vitro: vasculogenic mimicry, *Am. J. Pathol.* 155 (1999) 739–752.
- [25] S.C. Williamson, R.L. Metcalf, F. Trapani, S. Mohan, J. Antonello, B. Abbott, et al., Vasculogenic mimicry in small cell lung cancer, *Nat. Commun.* 7 (2016) 13322.
- [26] M.J. Hendrix, E.A. Sefror, A.R. Hess, R.E. Sefror, Vasculogenic mimicry and tumour-cell plasticity: lessons from melanoma, *Nat Rev Cancer* 3 (2003) 411–421.
- [27] L. Cheng, Z. Huang, W. Zhou, Q. Wu, S. Donnola, J.K. Liu, et al., Glioblastoma stem cells generate vascular pericytes to support vessel function and tumor growth, *Cell* 153 (2013) 139–152.
- [28] A.K. Shenoy, Y. Jin, H. Luo, M. Tang, C. Pampo, R. Shao, et al., Epithelial-to-mesenchymal transition confers pericyte properties on cancer cells, *J. Clin. Invest.* 126 (2016) 4174–4186.
- [29] A. Bellahcene, R. Bachelier, C. Detry, R. Lidereau, P. Clezardin, V. Castronovo, Transcriptome analysis reveals an osteoblast-like phenotype for human osteotropic breast cancer cells, *Breast Canc. Res. Treat.* 101 (2007) 135–148.
- [30] C.C. Tan, G.X. Li, L.D. Tan, X. Du, X.Q. Li, R. He, et al., Breast cancer cells obtain an osteomimetic feature via epithelial-mesenchymal transition that have undergone BMP2/RUNX2 signaling pathway induction, *Oncotarget* 7 (2016) 79674–79691.
- [31] A. Masszi, P. Speight, E. Charbonney, M. Lodyga, H. Nakano, K. Szaszi, et al., Fate-determining mechanisms in epithelial-myo-fibroblast transition: major inhibitory role for Smad3, *JCB (J. Cell Biol.)* 188 (2010) 383–399.
- [32] L.C. Huysentruyt, P. Mukherjee, D. Banerjee, L.M. Shelton, T.N. Seyfried, Metastatic cancer cells with macrophage properties: evidence from a new murine tumor model, *Int J Cancer* 123 (2008) 73–84.
- [33] I. Jatoi, S.G. Hilsenbeck, G.M. Clark, C.K. Osborne, Significance of axillary lymph node metastasis in primary breast cancer, *J. Clin. Oncol.* 17 (1999) 2334–2340.
- [34] H. Ji, R. Cao, Y. Yang, Y. Zhang, H. Iwamoto, S. Lim, et al., TNFR1 mediates TNF- $\alpha$ -induced tumour lymphangiogenesis and metastasis by modulating VEGF-C-VEGFR3 signalling, *Nat. Commun.* 5 (2014) 4944.
- [35] J.A. Park, D.Y. Kim, Y.M. Kim, I.K. Lee, Y.G. Kwon, Endothelial Snail regulates capillary branching morphogenesis via vascular endothelial growth factor receptor 3 expression, *PLoS Genet.* 11 (2015), e1005324.
- [36] S.L. Dagenais, R.L. Hartsough, R.P. Erickson, M.H. Witte, M.G. Butler, T.W. Glover, Foxc2 is expressed in developing lymphatic vessels and other tissues associated with lymphedema-distichiasis syndrome, *Gene Expr. Patterns* 4 (2004) 611–619.
- [37] X. Wu, N.F. Liu, FOXC2 transcription factor: a novel regulator of lymphangiogenesis, *Lymphology* 44 (2011) 35–41.
- [38] J.D. Kanady, S.J. Munger, M.H. Witte, A.M. Simon, Combining Foxc2 and Connexin37 deletions in mice leads to severe defects in lymphatic vascular growth and remodeling, *Dev. Biol.* 405 (2015) 33–46.
- [39] P.K. Lo, J.S. Lee, X. Liang, S. Sukumar, The dual role of FOXF2 in regulation of DNA replication and the epithelial-mesenchymal transition in breast cancer progression, *Cell. Signal.* 28 (2016) 1502–1519.
- [40] H.P. Tian, S.M. Lun, H.J. Huang, R. He, P.Z. Kong, Q.S. Wang, et al., DNA methylation affects the SP1-regulated transcription of FOXF2 in breast cancer cells, *J. Biol. Chem.* 290 (2015) 19173–19183.
- [41] Z.H. Yu, S.M. Lun, R. He, H.P. Tian, H.J. Huang, Q.S. Wang, et al., Dual function of MAZ mediated by FOXF2 in basal-like breast cancer: promotion of proliferation and suppression of progression, *Canc. Lett.* 402 (2017) 142–152.
- [42] W. Shi, K. Gerster, N.M. Alajez, J. Tsang, L. Waldron, M. Pintiile, et al., MicroRNA-301 mediates proliferation and invasion in human breast cancer, *Cancer Res.* 71 (2011) 2926–2937.
- [43] H. Hirata, K. Ueno, V. Shahyari, G. Deng, Y. Tanaka, Z.L. Tabatabai, et al., MicroRNA-182-5p promotes cell invasion and proliferation by down regulating FOXF2, RECK and MTSS1 genes in human prostate cancer, *PLoS One* 8 (2013), e55502.
- [44] Y.Z. Zheng, J. Wen, X. Cao, H. Yang, K.J. Luo, Q.W. Liu, et al., Decreased mRNA expression of transcription factor forkhead box F2 is an indicator of poor prognosis in patients with resected esophageal squamous cell carcinoma, *Mol Clin Oncol* 3 (2015) 713–719.